

DOI: 10.13208/j.electrochem.140603

Artical ID:1006-3471(2015)02-0172-09

Cite this: *J. Electrochem.* **2015**, 21(2): 172-180

Http://electrochem.xmu.edu.cn

Electrodeposition of Al-Mg Alloys from Acidic $\text{AlCl}_3\text{-EMIC-MgCl}_2$ Room Temperature Ionic Liquids

M. Rostom Ali^{1,2*}, Andrew P. Abbott¹, Karl S. Ryder¹

(1. *Department of Chemistry, University of Leicester, Leicester LE1 7RH, UK*; 2. *Department of Applied Chemistry and Chemical Engineering, University of Rajshahi, Rajshahi-6205, Bangladesh*)

Abstract: Electrodeposition of aluminium-magnesium alloys have been carried out onto platinum and copper cathodes from Lewis acidic aluminium(III) chloride-1-ethyl-3-methylimidazolium chloride ionic liquid containing magnesium(II) chloride by constant current and constant potential methods at room temperature. Magnesium content in the deposited alloy increases with increasing MgCl_2 concentration in the ionic liquid and with increasing cathodic current density. The influences of various experimental conditions on electrodeposition and the morphology of the electrodeposited layers have been investigated by X-ray diffraction (XRD) and scanning electron microscopy (SEM) equipped with energy dispersive X-ray spectroscopy (EDAX). On increasing the deposition current densities the dense, bright, adherent and smooth electrodeposited layers are obtained. The cathodic current efficiency for the deposition of Al-Mg alloys is about 99%. The electrochemical quartz crystal microbalance (EQCM) has been used to study alloy deposition. The composition of the metal co-deposit has been calculated from the slopes of the mass-charge (m - Q) plots of gravimetric acoustic impedance analysis.

Key words: electrodeposition; Al-Mg alloys; ionic liquids; cyclic voltammetry; constant potential

CLC Number: O646

Document Code: A

Magnesium (Mg) alloys offer a high potential for use as lightweight structural materials in automotive and aircraft applications in recent years. However, poor corrosion resistance has limited its usage in hostile environments^[1-3]. Therefore, aluminium (Al) has been selected as an alloying element for improving the corrosion resistance of the Mg alloys because it is lightweight, inexpensive and has high corrosion resistance. Aluminium-magnesium (Al-Mg) alloys have attractive properties, such as low density, high strength and work-hardening ability, and these accounts for their uses in wide variety of chemical-processing and food handling equipment as well as structural applications involving exposure to seawater. Coating these alloys on substrates offers similar property enhancements for surfaces.

There are various methods for Al coating such as, hot dipping, thermal spraying, sputter deposition, vapour deposition and electrodeposition. The electrodeposition process offers several advantages, namely, the deposits are usually adherent and do not affect the structural and mechanical properties of the substrate. Furthermore, the thickness and the quality of the deposits can be adjusted by controlling the experimental parameters, and it is cost-effective, since it is performed at moderate temperatures.

The electrodeposition of Al and its alloys is not possible from aqueous solutions because of its reactivity (-1.67 V vs. NHE). Therefore, electrolytes for the electrodeposition of Al and its alloys must be aprotic so that the complications associated with hydrogen evolution that occur in aqueous baths are

Received: 2014-06-03, Revised: 2014-07-28 *Corresponding author, Tel: +880-1727226745, E-mail: dmrli@yahoo.com

The authors gratefully acknowledge the Commonwealth Scholarship Commission and British Council in the UK for awarding the Commonwealth Post-Doc Staff Fellowship of one of us (RA) in 2008.

eliminated. The electrodeposition of Al in organic solutions is commercially available (SIGAL process)^[4]. However, due to volatility and flammability of the solvent use of the process has been largely abandoned. An alternative approach has been through the development of room temperature ionic liquids for Al electrodeposition. Many papers have been published on the electrodeposition of Al and its alloys from chloroaluminate, so-called first generation ionic liquids^[5-16]. These liquids are AlCl_3 -based ionic liquids and they are easy to be synthesized by simple addition of the Lewis acidic AlCl_3 to a 1, 3-dialkyl-imidazolium chloride, alkyl-pyridinium chloride, quaternary ammonium compound under an inert atmosphere. Aluminium can be quite easily be electrodeposited in these ionic liquids as well as Al-base alloys, such as Al-Co^[9], Al-Cr^[10], Al-Ni^[11], Al-Ti^[12], Al-Mo^[14], Al-Zr^[17].

The aim of the present work is to develop a coating of Al-Mg alloys on copper substrate by electrodeposition method from Lewis acidic AlCl_3 -1-ethyl-3-*m*-ethylimidazolium chloride ionic liquids containing MgCl_2 at room temperature.

1 Experimental

1.1 Chemicals

Anhydrous magnesium chloride (MgCl_2) powder (99.9%, Aldrich), 1-ethyl-3-methylimidazolium chloride (EMIC) crystalline (99.9%, Fluka), anhydrous aluminium chloride (AlCl_3 , 99.99%, Aldrich), toluene, methanol and acetone (Fisher Scientific UK Ltd.) were used in the present study.

1.2 Preparation of Ionic Liquids

All chemicals were handled under a nitrogen atmosphere in a glove box. Two acidic AlCl_3 -EMIC ionic liquids, 1.65:1 mole ratio (supplied by BASF) and 2:1 mole ratio (prepared in the laboratory) were used in all experiments. The ionic liquid of 2:1 molar ratio AlCl_3 to EMIC was prepared by slow addition of known weights of the two components in a vacuum glass bottle using a magnetic bar stirrer. Slight fogging was observed during preparation due to highly exothermic reaction between AlCl_3 and EMIC components, and care was taken to control the reaction rate and to avoid the decomposition of the elec-

trolytes. The resulting ionic liquid was then purified by placing under vacuum with some small pieces of pure aluminium (99.9%). The purification operation was carried out step wise until the ionic liquid became colourless. Acidic AlCl_3 -EMIC- MgCl_2 ionic liquid was prepared by heating the mixture of MgCl_2 and acidic AlCl_3 -EMIC ionic liquid at 70 °C with a magnetic bar stirrer. The concentrations of MgCl_2 (measured by ICP) in the 1.65:1 (mole ratio) and 2:1 (mole ratio) AlCl_3 -EMIC ionic liquids were 0.06 and 0.11 mol·L⁻¹, respectively.

1.3 Electrochemical Measurements

The electrolytic cell used in the present study was made of Pyrex glass with a fitted Pyrex glass cap. The reference electrode was separated from the secondary compartment, containing the working and counter electrodes, by a fine porosity glass frit. The cell cap was fitted with three tungsten wires and clips were attached at each end to facilitate the mounting of the secondary and reference electrodes in the respective compartments. About 12 cm³ of the ionic liquid was used for electrochemical study.

Platinum (Pt, 50 mm × 5 mm × 0.1 mm) or copper (Cu, 50 mm × 5 mm × 0.4 mm) and commercial grade Al (50 mm × 15 mm × 0.4 mm) plates were used as working and counter electrodes, respectively. A pure Al plate (40 mm × 3 mm × 0.4 mm) was used as a reference electrode and immersed in the 2:1 AlCl_3 -EMIC ionic liquid of the reference electrode compartment. The electrolyte level in the reference compartment was kept slightly higher than the bulk electrolyte. Electrochemical investigations including potential step chronoamperometry, chronopotentiometry and cyclic voltammetry were carried out using an AUTOLAB PGSTAT20 potentiostat/galvanostat (eco chemie, Holland) controlled by GPES software. All potentials in this work are quoted with respect to this Al|2:1 AlCl_3 -EMIC reference electrode which will be written as Al|Al³⁺ in this paper.

1.4 Deposition of Al-Mg Alloy

Aluminium-magnesium alloy deposition were carried out onto platinum and copper cathodes under constant current and constant potential methods from

acidic AlCl_3 -EMIC ionic liquids containing MgCl_2 at room temperature (25 ± 1 °C). The applied current densities and potentials for depositing in different plating operations were $-5.0 \sim -60.0 \text{ A} \cdot \text{m}^{-2}$ and $-0.20 \sim -0.70 \text{ V}$, respectively. Following each deposition, the resulting deposit was soaked firstly in toluene, then in methanol, and finally washed with acetone to remove the residual ionic liquids. The deposit was then thoroughly rinsed with de-ionized water and dried with cold air.

1.5 Deposit Characterization

The surface morphologies of the deposited samples were then examined with scanning electron microscope (XL 30 SEM, PHILIPS) and its auxiliary energy dispersive X-ray spectroscopy (EDAX). X-ray diffraction analysis was also performed with a Philips PW 1716 diffractometer using $\text{Cu } K_\alpha$ radiation (40 kV, 25 mA) to explore the crystal structure of the deposits. Inductively coupled plasma atomic emission spectrometry (JY Ultima 2 ICP-AES) was used to assess the elemental composition of the deposits after dissolving in hydrochloric acid. By comparing the mass of each deposit with the theoretical mass based on the total charge passed during the experiments, the current efficiency was determined for each deposition condition.

2 Results and Discussion

2.1 Voltammetric Study of MgCl_2 in 1.65:1 AlCl_3 -EMIC Ionic Liquids

The cyclic voltammograms recorded on a Pt electrode in 1.65:1:0.06 (mole ratio) AlCl_3 -EMIC- MgCl_2 ionic liquids at 25 °C with a scan rate of $1 \text{ mV} \cdot \text{s}^{-1}$ are shown in Fig. 1. The scan (solid line) towards negative direction consists of the first reduction wave C_1 with the current starting to increase at -0.29 V , which levels off at C_2 . The reverse scan consists of the first oxidation peak P_{a1} at 0.13 V and the second oxidation peak P_{a2} at 0.25 V . From XRD and EDAX analyses, only pure Al has been detected in the deposit obtained at a deposition potential of -0.30 V (from C_1) by constant potential method. Therefore, the increase of the negative currents in the first reduction wave (C_1 is obviously associated with the reduc-

tion of Al ions to metallic state^[7, 18].

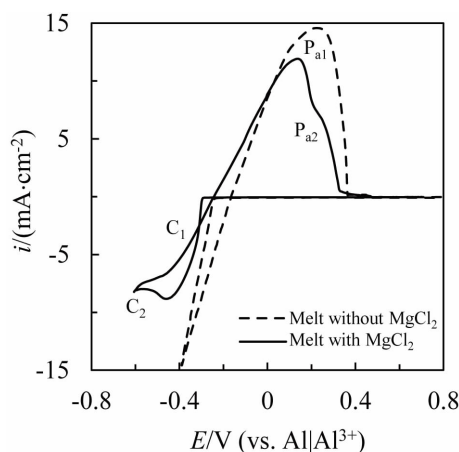
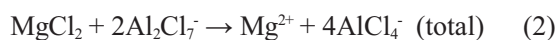


Fig. 1 Cyclic voltammograms recorded on a platinum electrode in 1.65:1 mole ratio AlCl_3 -EMIC ionic liquid containing $0.06 \text{ mol} \cdot \text{L}^{-1} \text{ MgCl}_2$ at 25 °C with a scan rate of $1 \text{ mV} \cdot \text{s}^{-1}$

Compared with the voltammograms obtained in the absence of MgCl_2 , the dotted curve in Fig. 1, the reduction wave appeared at -0.218 V corresponds to the reduction of Al species (Al_2Cl_7^-) and in the reverse scan a single symmetrical oxidation wave appeared at -0.164 V to the stripping of the deposited Al. When MgCl_2 is added into the ionic liquid, the deposition process is reduced such that the same deposition currents are obtained at more negative potentials than the ionic liquids without MgCl_2 .

Generally, in the Lewis basic ionic liquids most of the divalent metal ions exist in the form of a tetrahedral chloro-complex which is electro-inactive in metal electrodeposition process^[19-20]. However, in the acidic ionic liquids a bimetallic complex exists which is electro-active in a metal electrodeposition process^[19, 21]. If the divalent Mg ions exist as an uncomplex or octahedral coordinated state, then the concentration or activity of Al_2Cl_7^- ions in the bulk electrolyte will be decreased due to the formation of AlCl_4^- ions which can be represented according to the following solvation reaction.



Changing the ratio of Al_2Cl_7^- to AlCl_4^- leads to

the shift in the deposition potential of Al to more negative values than the ionic liquid without MgCl_2 . Therefore, it is concluded that the deposition of Al is suppressed by the addition of MgCl_2 since the addition of MgCl_2 into the 1.65:1 $\text{AlCl}_3\text{-EMIC}$ ionic liquid leads to the decrease in the concentration of Al_2Cl_7^- .

Fig. 2 shows the effect of cathodic sweeping potential on the cyclic voltammogram recorded on a Pt electrode in 1.65:1:0.06 (mole ratio) $\text{AlCl}_3\text{-EMIC-MgCl}_2$ ionic liquid at 25 °C with a scan rate of $1 \text{ mV} \cdot \text{s}^{-1}$. It is readily seen from the voltammograms that the first reduction wave C_1 corresponds to the first oxidation peak P_{a1} and the second reduction wave C_2 corresponds to the second oxidation peak P_{a2} . Therefore, the P_{a1} is attributed to the dissolution of the deposited Al from the similarity to the dotted curve in Fig. 1. When the potential sweep is made progressively more negative than -0.50 V, the P_{a2} begins to develop at about 0.40 V. From XRD analysis Al, Mg and $\text{Al}_{5.15}\text{Mg}_{3.15}$ intermetallic have been detected in the deposits obtained at a deposition potential -0.60 V (from C_2) by a constant potential method. ICP-AES showed that the Mg content increased from 1.8 to 3.1% (by mole) when the applied deposition potential is raised from -0.52 to -0.60 V. While this may not appear to be a significant amount, it is interesting to note that it is almost exactly the same mole ratio of Al:Mg in the ionic liquid. It is not possible to work at a higher concentration as the solution is effectively nearly saturated with MgCl_2 .

A brief study of this system has been carried out by Morimitsu et al. who obtained less than 2% Mg in the alloy and could not ascertain a separate Mg containing phase by XRD^[22]. It may be supposed that Al and Al-Mg alloys are deposited in the potential range below -0.50 V and the second oxidation peak corresponds to the dissolution of these alloys and intermetallic compounds. The formation of these alloy deposits can be represented according to the following general reaction, $0 < x < 1$.

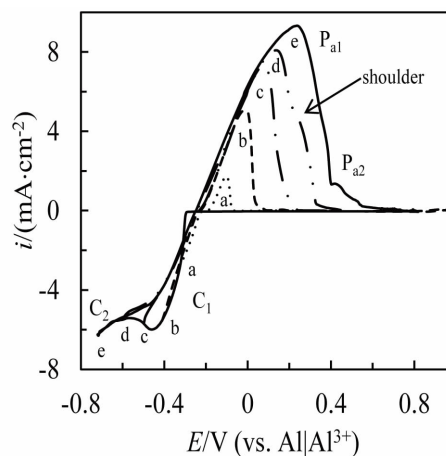
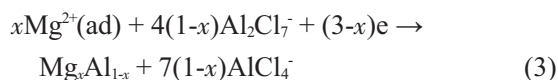


Fig. 2 Effect of sweeping potentials on the cyclic voltammograms recorded on a platinum electrode in 1.65:1:0.06 mole ratio $\text{AlCl}_3\text{-EMIC-MgCl}_2$ ionic liquid at 25 °C with a scan rate of $1 \text{ mV} \cdot \text{s}^{-1}$
Reverse potential: a. -0.31 V; b. -0.40 V; c. -0.50 V; d. -0.60 V; e. -0.70 V

Similar results have been reported for the deposition and dissolution of $\text{Al-Ni}^{[11, 23]}$, $\text{Al-Co}^{[9]}$ and $\text{Al-Cr}^{[10]}$ by several authors. Traces of pure Mg phase have been observed in the deposits obtained at an applied deposition current density of $-42 \text{ A} \cdot \text{m}^{-2}$ {Fig. 8A}. It can be concluded that Mg is predominantly deposited in the form of $\text{Al}_{5.15}\text{Mg}_{3.15}$. Under these conditions about 4% (by mole) Mg has been incorporated in the deposits.

2.2 Voltammetric Study of MgCl_2 in 2:1 $\text{AlCl}_3\text{-EMIC}$ Ionic Liquids

A series of cyclic voltammograms recorded on a Pt electrode in 2:1:0.11 (mole ratio) $\text{AlCl}_3\text{-EMIC-MgCl}_2$ ionic liquids at 25 °C as a function of cathodic sweeping potential with a scan rate of $1 \text{ mV} \cdot \text{s}^{-1}$ are shown in Fig. 3. At first glance the voltammograms for the two different ionic liquids appear similar, but overlaying the responses for the two liquids (Fig. 4) it is clear that there is a significant difference between the two systems. The onset potential of the first reduction process is more cathodic in the less Lewis acidic liquid. While this would be expected from simple Nernstian behaviour the magnitude of the difference c.a. 200 mV is more than expected by bulk concentration differences. This suggests that the dif-

ferences are due to the concentrations of the chloroaluminate species which are well documented^[24]. The magnitude of the cathodic current is smaller for the less Lewis acidic liquid as it contains less of the more easily reduced species (Al_2Cl_7^-). The dashed curve in Fig. 3 shows the voltammogram of 2:1 (mole ratio) AlCl_3 -EMIC ionic liquid, which is more reversible in nature as compared with 1.65:1 (mole ratio) AlCl_3 -EMIC ionic liquid.

From an XRD analysis, pure Al and $\text{Al}_{5.15}\text{Mg}_{3.15}$ intermetallic have been detected in the deposits obtained at a deposition potential of -0.40 V (from C_1) by constant potential method which is in contrast to the less Lewis acidic liquid where only Al has been detected. The solubility of MgCl_2 in the more Lewis acidic (2:1) mixture is almost double than that of the 1.65:1 melt and this is seen in approximately doubled increases in the amount of Mg incorporated in the alloy coatings.

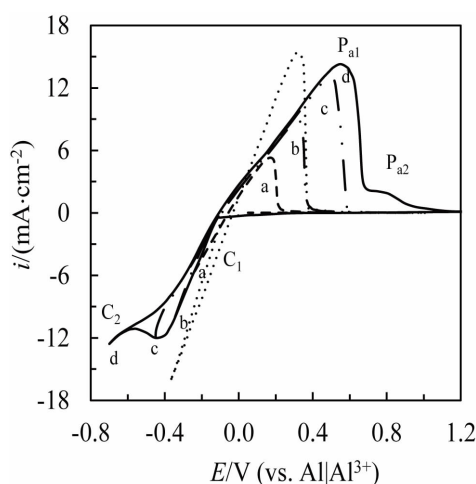


Fig. 3 Effect of sweeping potentials on the cyclic voltammograms recorded on a platinum electrode in 2:1:0.11 mole ratio AlCl_3 -EMIC- MgCl_2 ionic liquid at 25 °C with a scan rate of $1 \text{ mV} \cdot \text{s}^{-1}$
Reverse potential: a. -0.19 V; b. -0.30 V; c. -0.45 V; d. -0.60 V; e. -0.70 V; f. -0.83 V; (.....), ionic liquid without MgCl_2

2.3 Electrodeposition Study of Al-Mg Alloys

All the electrodeposits obtained are bright and good adherence. There is no rupture on the deposit surface and it does not peel off. Figs. 5 and 6 show

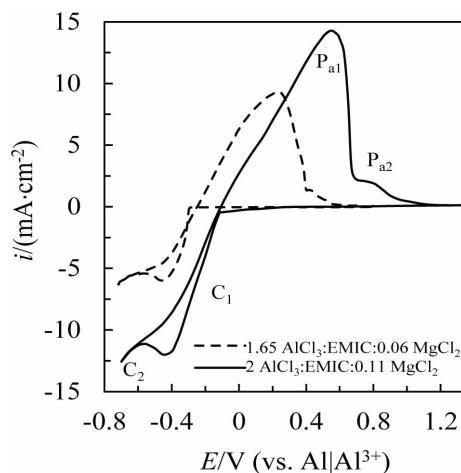


Fig. 4 Comparison of the cyclic voltammograms for 1.65:1:0.06 (dotted curve) and 2:1:0.11 (solid curve) mole ratio AlCl_3 -EMIC- MgCl_2 ionic liquids at 25 °C
Scan rate: $1 \text{ mV} \cdot \text{s}^{-1}$

the scanning electron micrographs of the electrodeposits obtained from 1.65:1:0.06 and 2:1:0.11 (mole ratio) AlCl_3 -EMIC- MgCl_2 ionic liquids, respectively. There is a significant difference between the morphology of the deposits obtained at the two different compositions. The more Lewis acidic liquid produces plate-like crystals at low current densities and overpotentials which grow perpendicular to the electrode surface. This morphology differs from Al deposited from the ionic liquid without MgCl_2 , suggesting that the Mg changes the morphology of the deposit. Identical plate-like crystals have, however, been seen for zinc deposition and these have been ascribed to differences in the double layer properties in the ionic liquid^[25]. Two-dimensional crystals are seen in liquids with a high chloride activity whereas nodular growth is observed when chloride activity is suppressed. The thicknesses of the deposited layers are in the range of $6 \sim 8 \mu\text{m}$, which has been controlled by adjusting the total charge applied.

In the 1.65:1:0.06 AlCl_3 -EMIC- MgCl_2 ionic liquid the sizes of the electrodeposited crystals at low current densities ($< -20 \text{ A} \cdot \text{m}^{-2}$) are angular in shape and in the order of $10 \sim 15 \mu\text{m}$ in size, which is the same in structure as pure Al^[24]. However, the sizes of the deposited particles between the range of deposition current densities from -20 to $-45 \text{ A} \cdot \text{m}^{-2}$ are nodular in

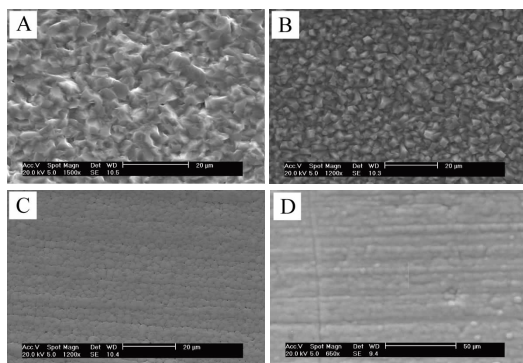


Fig. 5 SEM images of Al-Mg alloy electrodeposits on Cu substrate from 1.65:1:0.06 mole ratio $\text{AlCl}_3\text{-EMIC-MgCl}_2$ ionic liquid at 25 °C

A. -0.30 V; B. -0.50 V; C. $-33.3 \text{ A} \cdot \text{m}^{-2}$; D. $-42.0 \text{ A} \cdot \text{m}^{-2}$

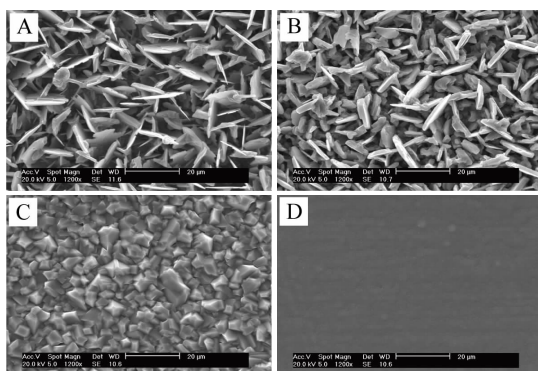


Fig. 6 SEM images of Al-Mg alloy electrodeposits on Cu substrate from 2:1:0.11 mole ratio $\text{AlCl}_3\text{-EMIC-Mg-Cl}_2$ ionic liquid at 25 °C

A. $-4.5 \text{ A} \cdot \text{m}^{-2}$; B. -0.35 V; C. -0.50 V; D. -0.60 V

shape and in the order of $4 \sim 5 \mu\text{m}$ in size. The deposits obtained at these conditions are very smooth, bright and also have good adherence. The deposited particles obtained above $-60 \text{ A} \cdot \text{m}^{-2}$ become finer. At low deposition current densities, the reductions of Al_2Cl_7^- and Mg containing species (either Mg^{2+} or $[\text{Mg}(\text{AlCl}_4)_3]$) occur slowly on the cathode. Consequently, the growth rate of nuclei is greater than the rate of formation of new nuclei and so the deposited particles should be large. As the deposition current densities increase, the formation of new nuclei is favoured and the particles become finer. Fig. 7 shows the EDAX profile for the SEM micrograph in Fig. 5A and 5D. Pure Al, and Al with Mg have been detected on the deposited layers by EDAX analysis. There is no spectrum for residual

chloride in the EDAX profile indicating no incorporation of the ionic liquid in the deposits.

The acquired diffraction patterns for the deposits obtained from molar ratios of 1.65:1:0.06 and 2:1:0.11 $\text{AlCl}_3\text{-EMIC-MgCl}_2$ ionic liquids at applied deposition potentials of -0.60 V and -0.40 V, respectively, are shown in Fig. 8A and 8B. The diffraction peaks at $2\theta = 38.5^\circ$, 44.7° , 65.1° , and 78.2° are for Al, while the peaks at 36.13° , 37.60° , and 43.69° for $\text{Al}_{5.15}\text{Mg}_{3.15}$ and the peaks at 36.64° , 47.83° , 57.55° for Mg. The diffraction peaks of the deposited layers are very sharp indicating that the deposits have crystalline structure. The deposits obtained at low current density have several crystal structures of Al with the dominant crystal structure of Al (111). However at high deposition current density, the dominant crystal structure of Al is (200). The current efficiencies for the deposition of pure Al and Al-Mg alloy are about 99%. However, additional diffraction peaks at $2\theta = 43.3^\circ$, 50.45° and 74.1° corresponding to Cu substrate are also observed in Fig. 8.

2.4 EQCM Studies on Gold

The composition of the metal co-deposit has been examined using gravimetric acoustic impedance methods. Usually this technique is most effective where the mass difference between the two metals is large, e.g. Cu and Ag or Zn and Sn. In this case the mass difference between Al and Mg is very small but the limiting slopes of the mass charge plots are easily distinguished on the basis of charge according to the Faraday relation, Equation (4):

$$\Delta m = \frac{\text{ram}\Delta Q}{nF} \quad (4)$$

where Δm is the change of electrode mass (in g), ram is the molar mass of the deposit (in g per mole), ΔQ is the change of the total electric charge that passes through the solution (in coulombs), n is the valence number of the substance as in solution (electrons per ion), F is the Faraday constant (in coulombs per mole).

For deposition of pure Al the theoretical slope for the mass charge plot is $\text{dm}/\text{d}Q = 9.328 \times 10^{-5} \text{ g} \cdot \text{C}^{-1}$ and for pure Mg $\text{dm}/\text{d}Q = 1.244 \times 10^{-4} \text{ g} \cdot \text{C}^{-1}$ (assuming that the current efficiencies for both processes are 100%). The total mass and charge balance of the co-

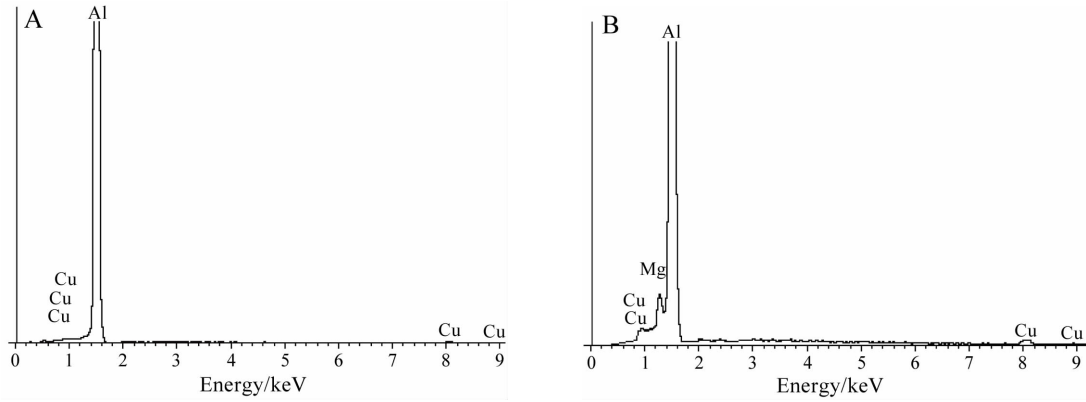


Fig. 7 EDAX profiles of the SEM images in Fig. 5A (left) and 5D (right)

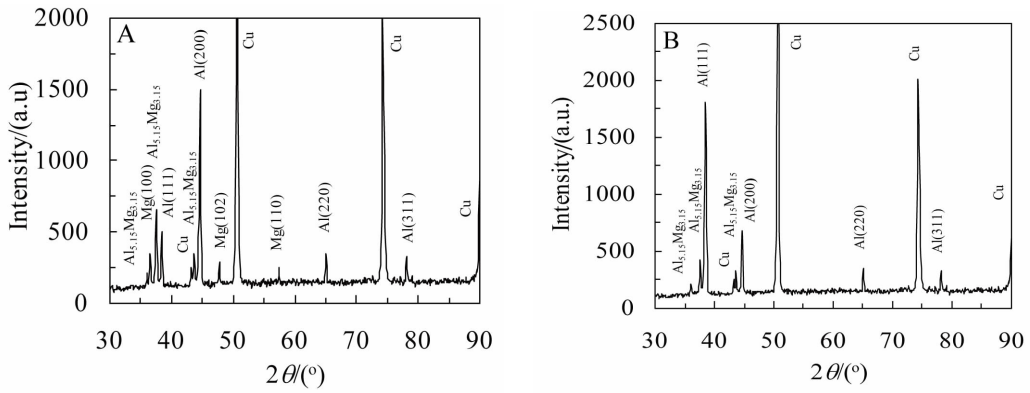


Fig. 8 X-ray diffraction patterns of the electrodeposited Al-Mg alloy

A. electrodeposited from 1.65:1:0.06 AlCl_3 -EMIC- MgCl_2 ionic liquid at -0.60 V; B. electrodeposited from 2:1:0.11 AlCl_3 -EMIC- MgCl_2 ionic liquid at -0.40 V

deposits during deposition can be represented by Equations (5) and (6).

$$\text{Mass}_{\text{Total}} = X_{\text{Mg}} \times \text{ram}_{\text{Mg}} + (1 - X_{\text{Mg}}) \times \text{ram}_{\text{Al}} \quad (5)$$

$$Q_{\text{Total}} = 2FX_{\text{Mg}} + 3F(1 - X_{\text{Mg}}) = F(3 - X_{\text{Mg}}) \quad (6)$$

These are easily combined to give an expression for the slope of the mass charge plot electrolytic deposition of the alloy/mixed phases, Equation (7), and this can be rearranged to give composition, Equation (8).

$$\frac{dm}{dQ} = \frac{X_{\text{Mg}} \text{ram}_{\text{Mg}} + (1 - X_{\text{Mg}}) \text{ram}_{\text{Al}}}{F(3 - X_{\text{Mg}})} \quad (7)$$

$$X_{\text{Mg}} = \frac{\text{ram}_{\text{Al}} - 3F \left(\frac{dm}{dQ} \right)}{\left(\text{ram}_{\text{Al}} - \text{ram}_{\text{Mg}} - F \left(\frac{dm}{dQ} \right) \right)} \quad (8)$$

This methodology has been applied to analyze the data from the electrolytic co-deposition of Mg and Al from a liquid containing 2:1 (mole ratio) AlCl_3 -EMIC and 0.11 moles of MgCl_2 . The deposition experiment

has been carried out at an applied potential of either -0.40 V or -0.60 V versus $\text{Al}|\text{Al}^{3+}$. Acoustic impedance spectra are recorded every second throughout the deposition period and these are fitted using numerical methods described elsewhere to extract the centre frequency and resonance Q factor (peak width). During the deposition experiment at $E = -0.40$ V the Q factor and peak intensity of the resonance varied from the initial values of 175 and $0.53 \Omega^{-1}$ to the final values of 143 and $0.42 \Omega^{-1}$, respectively. The corresponding values for the deposition at -0.60 V are 175 and $0.51 \Omega^{-1}$ initially to 164 and $0.40 \Omega^{-1}$ finally. These data show that viscoelastic effects are absent and, thus, frequency changes are correlated with mass using the Sauerbrey equation. The mass changes are converted into molar fraction data using Equation (8) and the results are presented in Fig. 9.

These data show that the composition of the de-

posit varies during the deposition from primarily Mg at short time and primarily Al at longer time. Deposition at low cathodic potentials (-0.40 V) favours Mg. This may be unexpected with the above results which show that Al is the main constituent but it is probably affected by the electrode material; gold, which readily forms alloys. This part of the study shows that Mg is kinetically rapid to be reduced (probably because of the electrode material) but mass transport causes the amount of Al in the alloy to increase with charge passed (and time). The films grown in Fig. 9 are 0.1 to $0.3\text{ }\mu\text{m}$ thick which is a factor of 10 times less than the films analysed following bulk electrolysis. This shows that electrolytically grown alloys are not homogeneous in the z -direction.

Analysis of results from a similar experiment from a liquid consisting of $1.65\text{AlCl}_3\text{:EMIC}$ gave values for molar fraction data that are consistently too high (i.e. > 1). This may be because of adsorption effects at the metal/solution interface resulting in the added mass without corresponding Faradaic charge. Whilst this is yet to be confirmed, it is known that the mechanism of electrolytic deposition of Al from these melts is strongly dependent on composition in so-called Lewis basic stoichiometries where the molar ratio of Al to EMIC < 2 .

3 Conclusions

The smooth, shiny and good adherent Al-Mg alloys can be electrodeposited on platinum and copper cathodes from acidic $\text{AlCl}_3\text{-EMIC}$ ionic liquids containing Mg(II) ions by constant current and constant potential methods at room temperature. The Mg content in the deposit increases with increasing concentration of MgCl_2 in the ionic liquid although the relatively poor solubility of MgCl_2 means that the Mg content of the alloy does not rise above 6% (by mass). The morphology of the deposited films varies with the change of the deposition current density. The deposits obtained between the deposition current densities of -20 and $-45\text{ A}\cdot\text{m}^{-2}$ are very smooth, bright with good adherence and uniform grain size.

Acknowledgments

The authors gratefully acknowledge the Commonwealth Scholarship Commission and British

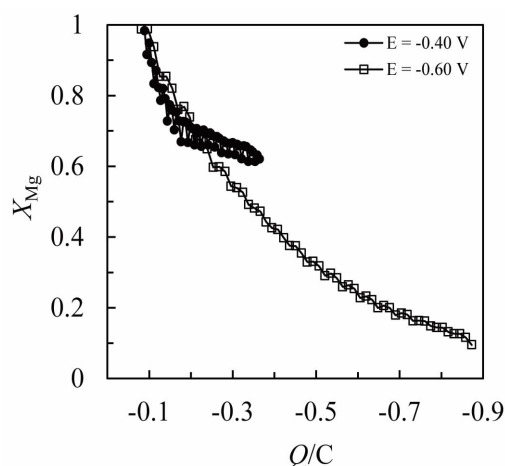


Fig. 9 Molar fraction of Mg incorporated into an Al-Mg alloy as a function of charge from a liquid containing $2\text{AlCl}_3\text{-EMIC}$ and 0.11 moles of MgCl_2 . Electrodeposited at -0.40 V and -0.60 V versus Al|Al^{3+} .

Council in the UK for awarding the Commonwealth Post-Doc Staff Fellowship of one of us (RA) in 2008.

References:

- [1] Makar G L, Kruger J. Corrosion studies of rapidly solidified magnesium alloys[J]. Journal of the Electrochemical Society, 1990, 137(2): 414-421.
- [2] Song G, Atrens A, John D St, et al. The anodic dissolution of magnesium in chloride and sulphate solutions[J]. Corrosion Science, 1997, 39(10/11): 1981-2004.
- [3] Ambat R, Aung N N, Zhou W. Evaluation of microstructural effects on corrosion behaviour of AZ91D magnesium alloy[J]. Corrosion Science, 2000, 42(8): 1433-1455.
- [4] Kautek W, Birkle S. Aluminum-electrocrystallization from metal-organic electrolytes[J]. Electrochimica Acta, 1989, 34(8): 1213-1218.
- [5] Zhao Y, Vander Noot T J. Electrodeposition of aluminum from room temperature $\text{AlCl}_3\text{-TMPAC}$ molten salts [J]. Electrochimica Acta, 1997, 42(11): 1639-1643.
- [6] Melton T J, Joyce J, Maloy J T, et al. Electrochemical studies of sodium chloride as a lewis buffer for room temperature chloroaluminate molten salts[J]. Journal of the Electrochemical Society, 1990, 137(12): 3865-3869.
- [7] Carlin R T, Osteryoung R A. Aluminum anodization in a basic ambient temperature molten salt[J]. Journal of the Electrochemical Society, 1989, 136(5): 1409-1415.
- [8] Moffat T P. Electrodeposition of $\text{Ni}_{1-x}\text{Al}_x$ in a chloroaluminate melt[J]. Journal of the Electrochemical Society, 1994, 141(11): 3059-3070.
- [9] Ali M R, Nishikata A, Tsuru T. Electrodeposition of Co-Al

- alloys of different composition from the AlCl_3 -BPC- CoCl_2 room temperature molten salt[J]. *Electrochimica Acta*, 1997, 42(12): 1819-1828.
- [10] Ali M R, Nishikata A, Tsuru T. Electrodeposition of aluminum-chromium alloys from AlCl_3 -BPC melt and its corrosion and high temperature oxidation behaviors [J]. *Electrochimica Acta*, 1997, 42(15): 2347-2354.
- [11] Ali M R, Nishikata A, Tsuru T. Electrodeposition of Al-Ni intermetallic compounds from aluminum chloride-N-(*n*-butyl)pyridinium chloride room temperature molten salt[J]. *Journal of Electroanalytical Chemistry*, 2001, 513(2): 111-118.
- [12] Ali M R, Nishikata A, Tsuru T. Electrodeposition of Al-Ti alloys from aluminum chloride-N-(*n*-butyl)pyridinium chloride room temperature molten salt[J]. *Indian Journal of Chemical Technology*, 2003, 10(1): 14-20.
- [13] Stafford G R. The electrodeposition of Al_3Ti from chloroaluminate electrolytes[J]. *Journal of the Electrochemical Society*, 1994, 114(4): 945-953.
- [14] Tsuda T, Hussay C L, Stafford G R. Electrodeposition of Al-Mo alloys from the lewis acidic aluminum chloride-1-ethyl-3-methylimidazolium chloride molten salt[J]. *Journal of the Electrochemical Society*, 2004, 151(6): C379-C384.
- [15] Stafford G R. The electrodeposition of an aluminum-manganese metallic glass from molten salts[J]. *Journal of the Electrochemical Society*, 1989, 136(3): 635-639.
- [16] Endres F, Bukowski M, Hempelmann R, et al. Electrodeposition of nanocrystalline metals and alloys from ionic liquids [J]. *Angewandte Chemie International Edition*, 2003, 42(29): 3428-3430.
- [17] Tsuda T, Hussay C L, Stafford G R, et al. Electrodeposition of Al-Zr alloys from lewis acidic aluminum chloride-1-ethyl-3-methylimidazolium chloride melt[J]. *Journal of the Electrochemical Society*, 2004, 151(7): C447-C454.
- [18] Lai P K, Kazacos M S. Electrodeposition of aluminium in aluminium chloride/1-methyl-3-ethylimidazolium chloride[J]. *Journal of Electroanalytical Chemistry*, 1988, 248(2): 431-440.
- [19] Hussey C L, Laher T M. Electrochemical and spectroscopic studies of cobalt(II) in molten aluminum chloride-N-(*n*-butyl)pyridinium chloride[J]. *Inorganic Chemistry*, 1981, 20: 4201-4206.
- [20] Hussey C L. Room temperature haloaluminate ionic liquids. Novel solvents for transition metal solution chemistry[J]. *Pure & Applied Chemistry*, 1988, 60(12): 1763-1772.
- [21] Abdul-sada A L, Greenway A M, Seddon K R, et al. Fast atom bombardment mass spectrometric evidence for the formation of tris {tetrachloroaluminate (III)} metallate (II) anions, $[\text{M}(\text{AlCl}_4)_3]^-$, in acidic ambient-temperature ionic liquids[J]. *Organic Mass Spectrometry*, 1992, 27(5): 648-649.
- [22] Morimitsu M, Tanaka N, Matsunaga M. Induced codeposition of Al-Mg alloys in lewis acidic AlCl_3 -EMIC room temperature molten salts[J]. *Chemistry Letters*, 2000, 29(9): 1028-1029.
- [23] Pitner W R, Hussey C L, Stafford G R. Electrodeposition of nickel-aluminum alloys from the aluminum chloride-1-methyl-3-ethylimidazolium chloride room temperature molten salt[J]. *Journal of the Electrochemical Society*, 1996, 143(1): 130-138.
- [24] Abbott A P, Qiu F, Abood H M A, et al. Double layer, diluents and anode effects upon the electrodeposition of aluminium from chloroaluminate based ionic liquids[J]. *Physical Chemistry Chemical Physics*, 2010, 12(8): 1862-1872.
- [25] Barron J C. Zn and its alloy electrodeposition from deep eutectic solvents[D]. University of Leicester, UK, 2009.

采用 AlCl_3 -EMIC- MgCl_2 室温离子液体 电沉积制备铝-镁合金

M. Rostom Ali^{1,2*}, Andrew P. Abbott¹, Karl S. Ryder¹

(1. 莱斯特大学化学系, 莱斯特 LE1 7RH, 英国; 2. 拉杰沙溪大学应用化学与化工系, 拉杰沙溪-6205, 孟加拉共和国)

摘要: 采用恒电流和恒电位技术, 以及路易斯酸氯化铝(III)-1-乙基-3-甲基咪唑氯化物离子液体中添加氯化镁(II), 室温下在铂和铜阴极表面电沉积制备了铝-镁合金。合金层中镁的含量随离子液体中氯化镁浓度和所施加的阴极电流密度的增加而增加。采用 X-射线衍射谱(XRD)、扫描电子显微镜(SEM)和能量散射 X-射线谱(EDAX)技术, 研究了不同电沉积实验条件得到的电沉积层的晶体结构及表面形貌。增加沉积电流密度, 可以制备出致密、光亮和结合力良好的电沉积层。铝-镁合金电沉积的阴极电流效率可达 99%。应用电化学石英晶体微天平(EQCM)技术研究了电沉积合金的组成。根据重声阻抗分析得到的质量-电荷(m - Q)曲线斜率计算了金属共沉积层的化学成分。

关键词: 电沉积; 铝-镁合金; 离子液体; 循环伏安; 恒电位